W. S. Kowalik*
US Geological Survey
Denver, CO 80225
R. J. P. Lyon
Dept. of Applied Earth Sciences
Stanford University
Stanford, CA 94305
P. Switzer
Dept. of Statistics
Stanford University
Stanford, CA 94305

The Effects of Additive Radiance Terms on Ratios of Landsat Data

The model predicts that a residual surface orientation effect is present in raw ratios of Landsat data due primarily to the additive path radiance term.

Abstract: *We use a simple equation describing the radiance measured in the visible and near infrared wavelength region by a satellite over a Lambertian surface to model the effects of the additive path radiance and skylight irradiance terms in ratios of Landsat data. Results from the model show that the path-radiance and skylight terms cause ratio values (with longer wavelengths in numerator) to increase when proceeding from poorly illuminated to well illuminated topographic slopes of the same surface material. A path radiance correction subdues the surface orientation effect and produces ratio values which are more directly related to the surface reflectance characteristics and less dependent upon the surface topographic orientation. Surface types with similar reflectance properties, but having different preferred topographic orientations, may be better separated with raw ratio values because the raw ratio values have an inherent topographic dependency.*

We test the predictions from the model in a mineral exploration framework by linear discriminant analyses using ratio variables on a sample of 183 sites on each of six Landsat data sets from the Yerington District of western Nevada. After a path radiance correction, the classification rate in the discrimination of limonite quartz monzonite from nonlimonitic areas increased by an average of 10 percent for the six data sets, from 87 percent to 97 percent. The improved rate after path radiance correction is due to the correct classification of sites that, according to the model, have potential for misclassification in raw data because of their topographic orientations.

Introduction

The effects of atmospheric and solar illumination conditions during imaging have not been very well understood in the application of Landsat data to mineral exploration. Most research involving the atmospheric correction of Landsat data has been in agricultural applications where surface topography is fairly flat and the solar illumination is therefore fairly uniform. Researchers have concentrated on the extension of signatures based upon measured brightness to other areas of an image, and to other images recorded under different atmospheric and illumination conditions.

Mineral exploration, on the other hand, is often conducted in mountainous terrain where illumination conditions can vary appreciably from one picture element (pixel) to another due to surface topography. The problem of variable illumination has been partly resolved in mineral exploration by the use of ratio variables—combinations of two or

* Now with the Chevron Oil Field Research Co., P.O. Box 446, La Habra, CA 90631.

Photogrammetric Engineering and Remote Sensing,
Vol. 49, No. 5, May 1983, pp. 659-669.

0099-1112/83/4905-0659$02.25/0

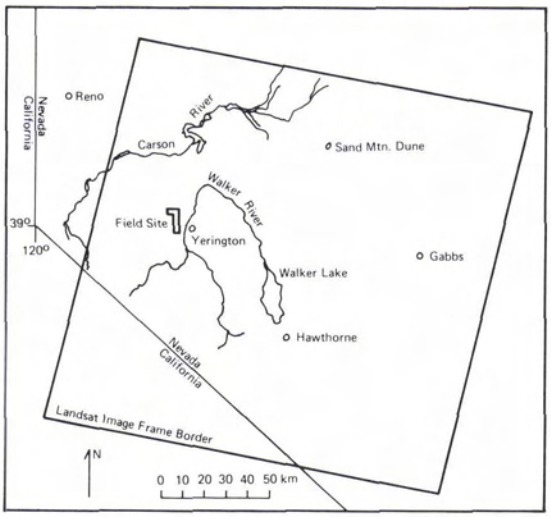

FIG. 1. Location map of western Nevada showing the field site area, the town of Hawthorne, Walter Lake, and the Sand Mountain dune.

more brightness (band) variables; e.g., Smedes *et al.* (1971), Vincent (1973), and Rowan *et al.* (1974).

We use a simple model for the radiance recorded by Landsat to predict several effects of the additive atmospheric radiance terms upon ratio variables in a geological context. Subsequently, we evaluate the predictions from the model by analyzing classification results from linear discriminant analyses. These analyses use Landsat data from 183 sites in the Yerington porphyry copper district of western Nevada (Figure 1) on each of six different images (Table 1).

Model of Radiance Recorded by Satellite

Equation 1 describes the radiance measured in a single wavelength band in the visible and near infrared region by a satellite with a vertically viewing sensor. The equation is based in part on Rogers and Peacock (1973), Reeves (1975, p. 91), Turner (1975), Rowan *et al.* (1977), Otterman *et al.* (1980), and Robinove and Chavez (1978):

$$L_c = \frac{S_c T_c P_c \, (Hd_c \cos \alpha + Hsky_c)}{\Pi} + S_c \, (Lpa_c + Lps_c) - S_c \, (OF_c) \qquad (1)$$

where the subscript c refers to a single wavelength band; the Landsat bands 4, 5, 6, and 7 are, respectively, 0.5 to 0.6 μm (green), 0.6 to 0.7 μm (red), 0.7 to 0.8 μm (near infrared), and 0.8 to 1.1 μm (near infrared); and

L_c = radiance measured by the satellite from one pixel, in integer units of Digital Number (DN, 7-bit, 0-127 scale);

S_c = the gain factor of satellite system (DN/radiance units = DN/mw/cm^2 sr);

TABLE 1. LANDSAT DATA SETS COVERING THE YERINGTON DISTRICT THAT WERE USED TO EVALUATE THE MODEL PREDICTIONS

Date	Image ID Number	Sun Elevation (°)
9/16/72	1055-18053	46
5/26/73	1307-18062	61
6/1/77	2861-17342	56
8/10/77	2951-17293	45
10/5/77	2987-17272	36
11/10/77	6023-17254	25

T_c = the vertical transmittance of the atmosphere from ground to satellite (dimensionless);

Hd_c = the direct illumination upon a surface at the bottom of the atmosphere and perpendicular to the sun vector (mw/cm^2);

$Hsky_c$ = the illumination due to skylight upon the surface (mw/cm^2);

$\cos \alpha$ = the surface orientation term (dimensionless); α is the angle between the sun vector and the perpendicular to the surface;

P_c = the surface reflectance; the ratio of the reflected energy to the incident energy; assuming Lambertian reflectance properties; i.e., P/Π sr units of the irradiance are assumed to be reflected;

Lpa_c = the radiance contributed by the atmospheric path; these are photons which never reached the Earth's surface but were instead scattered by the atmosphere into the sensor (mw/cm^2 sr); the path radiance decreases with increase in wavelength from the visible to the near infrared according to a $(1/\lambda)^{-4}$ to $(1/\lambda)^{-1}$ law (Slater, 1980);

Lps_c = the radiance contributed by the surface which is outside the instantaneous field of view of the sensor; these are photons which were reflected from the Earth's surface and were scattered by the atmosphere into the sensor (mw/cm^2 sr); and

OF_c = the offset value above which the radiance measured by a sensor is calibrated to read positive digital number units (mw/cm^2 sr).

The atmospheric and irradiance parameters in Equation 1 vary gradually in time and space (see

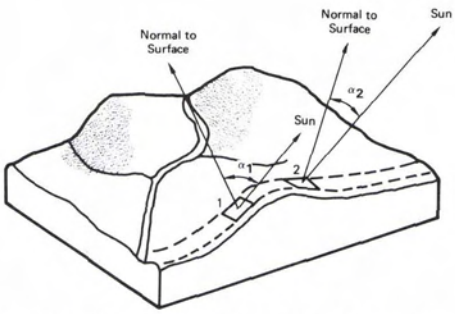

FIG. 2. Block model of a topographic surface showing two pixels with different topographic orientations. The angle α is the angle between the sun vector and the normal to the topographic surface at each pixel. Pixel 1 has a smaller cos α than does pixel 2. The angle α is related to the surface slope(s), solar zenith angle (z), and azimuth angle (t) by the following relation:

$$\alpha = \cos^{-1}(\cos s \cos z + \sin s \sin z \cos t),$$

where the azimuth angle (t) is the difference between the solar azimuth and azimuth of surface dip, measured clockwise from North.

Malila *et al.*, 1976), but for the purposes of our model, we hold them constant, and instead study the effects on ratios due to the P_c and cos α terms which vary much more rapidly in the spatial context. The P_c term contains the information about the surface that is of interest here, and cos α describes the variation in surface topography which modifies the radiance recorded by the satellite as shown in Equation 1.

VARIATION IN SURFACE TOPOGRAPHY

The orientation of the surface topography with respect to the solar elevation and azimuth angles affects the brightness measured by Landsat via the cos α term in Equation 1. Alpha (α) is the angle between the sun vector and the perpendicular to the surface (Figure 2). Cos α thus varies from 1.00 to 0.00 and lower to negative values. A site with a cos α of 1.00 faces directly into the incoming direct sunlight. A site with lower cos α is less well illuminated, and a site with cos α = 0.00 is grazingly illuminated by the direct sunlight. Sites with negative cos α values are shaded from the direct sunlight and are illuminated only by the skylight. Because cos α can range across a wide spread of values in hilly terrain, the brightness information recorded by the satellite tends to be proportional to P_c cos α, not to P_c.

Figure 3 shows the cos α distribution of the 183 field sites from the Yerington District on each of our six different Landsat data sets (Table 1). The six Landsat images cover a range of sun elevation angles from 61° to 25°. Notice that the cos α distribution for the field sites spans a larger range at

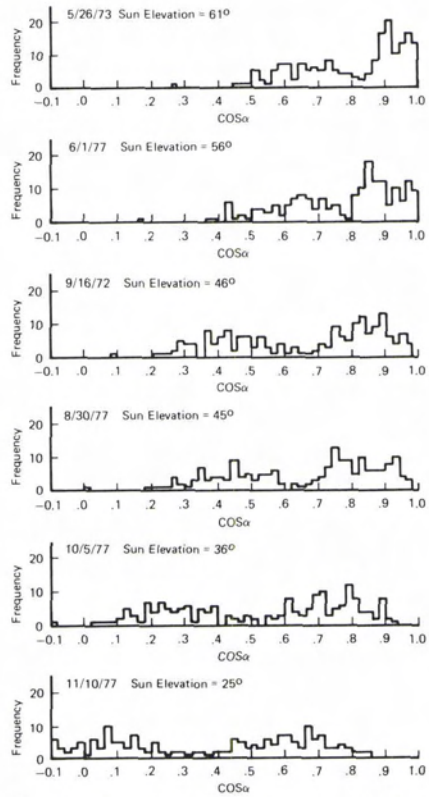

FIG. 3. Distributions of cos α for 183 field sites on each of six different Landsat overpasses of Yerington District, Nevada.

lower sun elevation angle. The tendency toward a bimodal distribution at lower sun elevation angle is caused by the NNE trend of topography in the Yerington District. At low sun angle, there is a wider disparity of cos α between the well illuminated ESE-facing and the poorly illuminated WNW-facing topographic surfaces.

Ratio variables are commonly used to enhance subtle rock type differences and to suppress the topographic brightness by cancellation of the cos α term. Various workers, including Kriegler *et al.* (1969), Vincent (1973), Rowan *et al.* (1974), and Chavez and Mitchell (1977), have noted that the topographic effect is not entirely removed from ratio values unless the path radiance term is first eliminated. The algebraic result of ratioing raw[1] DN values is given by Equation 2. In this case, cos α does not cancel algebraically[2]:

[1] The term "raw" is used throughout to define band brightness data which have not been corrected for the path radiance or skylight terms.

[2] In the following equations, the terms Lpa_c and Lps_c of Equation 1 have been combined into Lp_c for convenience because both are held constant.

$$\frac{L_1}{L_2} = \frac{\dfrac{S_1 T_1 P_1 (Hd_1 \cos \alpha + Hsky_1)}{\Pi} + S_1 (Lp_1 - OF_1)}{\dfrac{S_2 T_2 P_2 (Hd_2 \cos \alpha + Hsky_2)}{\Pi} + S_2 (Lp_2 - OF_2)} . \quad (2)$$

If a path radiance (and offset) correction is applied prior to ratioing by subtracting the appropriate band-dependent values from numerator and denominator, then we have the following:

$$\frac{L_1 - S_1 (Lp_1 - OF_1)}{L_2 - S_2 (Lp_2 - OF_2)} = \frac{S_1 T_1 P_1 (Hd_1 \cos \alpha + Hsky_1)}{S_2 T_2 P_2 (Hd_2 \cos \alpha + Hsky_2)} . \quad (3)$$

The surface orientation term has still not cancelled because of the additive skylight effect.

A skylight correction can be applied by evaluating the irradiance terms in the numerator and denominator and inverting, as given in Equation 4:

$$\frac{[L_1 - S_1 (Lp_1 - OF_1)] (Hd_2 \cos \alpha + Hsky_2)}{[L_2 - S_2 (Lp_2 - OF_2)] (Hd_1 \cos \alpha + Hsky_1)} = \frac{S_1 T_1 P_1}{S_2 T_2 P_2} . \quad (4)$$

The quantity on the right side of Equation 4 is independent of the surface orientation and is linearly proportional to the reflectance ratios.

Notice that, if cos α data and irradiance values were available from an auxiliary source, variables proportional to absolute reflectance could be derived as in Equation 5 without ratioing two bands: i.e.,

$$\frac{L_c - S_c (Lp_c - OF_c)}{Hd_c \cos \alpha + Hsky_c} = \frac{S_c T_c P_c}{\Pi} . \quad (5)$$

To apply the skylight correction in practice requires that the direct sunlight, skylight, and cos α values be known for each pixel. Thus, the cos α term cannot be strictly removed unless it and the irradiance terms are known from ancillary data. However, if the additive path radiance and skylight terms are small enough, cos α may effectively cancel. In common practice with Landsat data, cos α and the irradiance terms are not known, and ratios are created by Equations 2 or 3. Our results show that, when the surfaces of interest are spectrally different, Equation 3 (path radiance and offset correction) is preferred over Equation 2. We are not concerned here with methods for obtaining estimates of the band-dependent atmospheric path radiance values. For descriptions of such methods, refer to Chavez (1975), Chavez and Mitchell (1977), Switzer *et al.* (1981), or Kowalik (1981).

Modeled Effects of Surface Topography upon Ratio Values

We evaluate Equations 2 and 3 as a function of cos α to model the effects of the additive path radiance and skylight terms upon ratio values. We use Landsat in-band reflectance values for four different rock types in the modeling, and vary cos α from 0.0 to 1.0.

The four rock types are of geologic importance in the Yerington District (Figure 1). They are limonitic quartz monzonite (Lqm), nonlimonitic granodiorite (Ngd), hematitic tuff (Ht), and albitic quartz monzonite (Aqm). (See Knopf (1918), Moore (1969), and Proffett (1977) for a description of the geology of the District.)

The goal of the modeling is to help understand effects that the additive radiance terms have on our ability to spectrally distinguish between groups of these rock types with ratios of Landsat data. The Lqm and Ht rock types have a strong ferric absorption band centered in the ultraviolet which causes a rapid decrease in reflectance from the near infrared through the blue wavelength region (Hunt *et al.*, 1971). For the purposes of this paper, we concentrate on two Landsat ratios, 5/4 (red/green) and 6/4 (near infrared/green), that are affected by this absorption feature. The Lqm and Ht rock types have 5/4 and 6/4 ratios that are larger than the corresponding ratios for the Ngd and Aqm rock types.

The other four ratios of Landsat data (7/4, 7/5, 7/6, and 6/5) show modeled effects due to the path radiance and skylight that are smaller and similar in trend (Kowalik, 1981) to the results presented here for the 5/4 and 6/4 ratios. The 7/6 ratio is least affected by atmospheric scattering in the semi-arid terrain conditions modeled here, and is also useful for discriminating between rock types because of a ferric absorption band in the 0.8 to 0.9 μm region within Band 7 (Hunt and Ashley, 1979).

TABLE 2. PARAMETERS USED TO MODEL RATIO VALUES AS A FUNCTION OF COS α. THE PATH RADIANCE TERMS Lpa_c AND Lps_c ARE COMBINED HERE AS Lp_c.

Band	Hd $\left(\frac{(mw)}{(cm^2)}\right)$	Hsky $\left(\frac{(mw)}{(cm^2)}\right)$	T	Path Radiance minus Offset $S_c(Lp_c - OF_c)$ (DN)	System Gain $\left(\frac{(DN\ cm^2\ sr)}{(mw)}\right)$
4	13.55	1.31	0.68	11.9	49.80
5	17.32	1.32	0.75	7.0	74.71
6	13.13	0.84	0.76	3.4	86.99
7	16.44	1.00	0.77	0.0	33.42*

Reflectance Values:

Band	Limonitic quartz monzonite	Non-limonitic granodiorite	Hematitic tuff	Albitic quartz monzonite
4	0.129	0.183	0.118	0.208
5	0.182	0.216	0.150	0.236
6	0.204	0.253	0.180	0.271
7	0.214	0.284	0.196	0.291
Cosα	0.82	0.88	0.83	0.86

* The Band 7 gain was multiplied by 2 to increase the range to the 0-127 scale (USGS, 1979).

PARAMETERS USED IN MODEL

Our results from the model are based on parameters which approximate the conditions on 1 June 1977 during imaging of the western Nevada area by Landsat-2 (Table 2). We obtained these parameters as follows:

- The irradiance values were measured by Marsh (1978) with an Exotech Model 100 radiometer at Hawthorne, Nevada (location in Figure 1) during the overpass on 1 June 1977. The total irradiance (H_{total}) in each band was first measured with diffusing disks over the apertures and the radiometer oriented vertically upward. The skylight irradiance was then measured by shading the sun and aureole from the radiometer's field of view. The direct irradiance was calculated from the total and skylight irradiance by assuming that

$$H_{total\ c} = Hd_c \cos Z + Hsky_c$$

  where Z is the solar zenith angle.
- The atmospheric transmittance values were obtained from the Lowtran-4 atmospheric model program (Selby *et al.*, 1978) for a mid-latitude summer atmosphere and 56-degree sun elevation angle (6/1/77 overpass angle).
- The atmospheric path radiances were estimated from the Landsat-2 data recorded on 6/1/77 by the Covariance Matrix Method (Switzer *et al.*, 1980). The Covariance Matrix Method yields estimates of the path radiance minus the system offset term for each band in DN units. The estimates so derived minimize the variation in ratio values due to topography for the sample of pixels from the Yerington District that was passed through the algorithm.
- The system gain and offset factors for Landsat-2 are from USGS (1979).
- The reflectance values of the four sites listed in Table 2 are representative of these rock types at Yerington, Nevada, and were obtained from the satellite digital data by linear interpolation based on two known reflectance standards, the Sand Mountain Dune and Walker Lake (see location in Figure 1). This method of reflectance estimation has been successfully used by Lyon *et al.* (1975), Ballew (1975), and Marsh (1978), among others. The pixels corresponding to the four rock types used in modeling were located in the Landsat data by registering a gray scale dot matrix image at 1:24,000 scale (Ballew and Lyon, 1977) to a USGS orthophotoquad. We estimate that the sites are located in the Landsat data to $\pm$½ pixel. Because the four field sites were not horizontal, the "reflectance" values obtained by the conversion were normalized back to a horizontal orientation by multiplying the "reflectance" by (cos Z/cos α) for each of the four sites. The angle α is known from field measurements of surface orientation at each of the four sites and from the known solar position. Cos α values for each of these four sites during the 1 June 1977 overpass are listed in Table 2.

Equation 1 was initially evaluated with the atmospheric parameters listed in Table 2 for ten additional sites of known reflectance in western Nevada to provide a check upon the usefulness of the model. The reflectances of the ten other sites had been measured in the field by Marsh (1978) and Kowalik *et al.* (1980). The predicted digital number values are smaller than the values mea-

sured by Landsat-2 on 1 June 1977 by average factors of 1.7, 1.2, 1.2, and 2.1, respectively, in Bands 4, 5, 6, and 7. The standard deviations of these factors are small (0.1, 0.1, 0.1, 0.2), and indicate that the differences between the predicted and measured values are consistent among the ten sites.

The predicted digital numbers for Bands 5 and 6 are not too different from those actually measured, but Bands 4 and 7 are distinctly lower than those actually present on the Landsat-2 computer compatible tape (CCT). The 2.1 factor of Band 7 is suspiciously near 2.0. The Band 7 digital numbers obtained from the Landsat-2 CCT had been previously multiplied by 2 according to our usual processing convention, and the system gain for Landsat-2 was also multiplied by 2 to conform with the DN range change from 0-63 to 0-127 (USGS, 1979). Another factor of 2 was required to adjust the predicted DN values to those actually measured.

The differences between the predicted and measured DN values may be due to a combination of errors in the multiplicative system gain factor, the atmospheric transmittance, and the irradiance values. It is not possible to locate the errors with only one Landsat data set for which irradiance data are available (1 June 1977). However, we do not suspect that our model is at fault because the radiance values predicted by our model in physical units of mw/cm² sr (Kowalik, 1981) are similar to Landsat in-band radiances calculated by Malila *et al.* (1976) for various soil surfaces. A large share of the discrepancy in DN units for Bands 4 and 7 seems due to the use of pre-launch system gain factors. Malila *et al.* (1976) also had reason to suspect that the system gain factors determined by a pre-launch calibration for Landsat-1 were not valid after the launch.

Accordingly, the DN values predicted by our model have been enlarged by the above factors to yield DN values more similar to those actually measured by Landsat-2 on 1 June 1977. The modeled results which follow incorporate these multiplicative adjustment factors.

Because of uncertainty in the system gain factors, and because of different transmittance, irradiance, and scattering properties under other atmospheric and illumination conditions, the absolute values of the ratios calculated by the model (Figures 4 and 5) are not fixed. Rather, ratio values from the Landsat bands will be consistent in trend as a function of cos α to those shown, albeit of greater or lesser range, under other atmospheric, illumination, and reflectance conditions.

RESULTS FROM THE MODEL

Figure 4 shows the modeled variation in the raw and path radiance corrected (PRC) 5/4 ratio as a function of cos α for the four rock types. In raw mode, each rock type has a 5/4 value that increases in value toward larger cos α. The raw 6/4 ratio shows a similar increase in ratio values toward high cos α (Figure 5). In the modeled results, each rock type yields progressively larger ratio values as the surface topographic orientation shifts toward better illuminated positions. That is, the rocks appear to reflect relatively more of the longer wavelength light when facing into the sun (high cos α) than when facing away from the sun (low cos α). This effect is caused by the additive radiance terms in the model. The reflectance of each surface in the model does not change and remains the same at all surface orientations. Thus, the surface orientation adversely affects the spectral character of the surface which the analyst attempts to gauge by study of the raw ratio values. A simple plot of ratio values of Landsat data from a scan line traverse of 13 pixels across the Sand Mountain dune (Figure 6, location of dune is

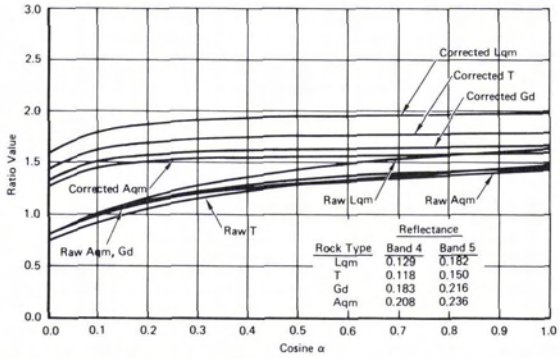

FIG. 4. Modeled 5/4 ratios as a function of cos α for four different rock types in the Yerington District: limonitic quartz monzonite (Lqm), nonlimonitic granodiorite (Gd), hematitic tuff (T), and albitic quartz monzonite (Aqm). The two sets of curves show the ratio values predicted by the model before and after a path radiance correction.

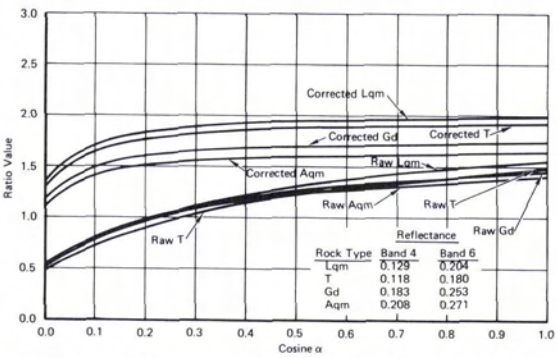

FIG. 5. Modeled 6/4 ratios as a function of cos α for the same rock types as in Figure 4. The two sets of curves show the ratio values predicted by the model before and after a path radiance correction.

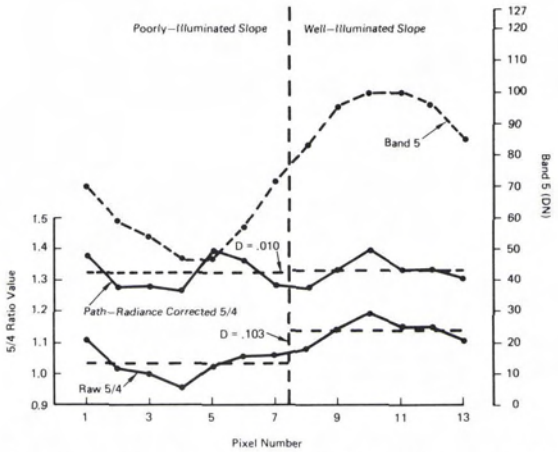

FIG. 6. Profile of Landsat-1 data from a traverse of 13 pixels across the Sand Mountain dune, Nevada. The dune is 120 m in height and 700 m across the base along the traverse. The diagram shows the Band 5 data, the raw 5/4 ratios, and the path radiance corrected 5/4 ratios. The horizontal dashed lines mark the mean ratio values on the well illuminated and poorly illuminated sides of the dune. After path radiance correction, the difference (D) in the mean 5/4 ratio value between both sides of the dune is 10× smaller than before correction. (Landsat image 1055-18053, sun elevation 46°.)

shown in Figure 1) upholds the basic form of Figures 4 and 5. The Landsat 5/4 ratio values are larger on the well-illuminated slope of the dune and are smaller on the northwest-facing, poorly illuminated side of the dune (Figure 6). The dune is unvegetated and is fairly homogeneous along the traverse. The variation in ratio values shown in Figure 6 is related to the topography of the dune, not to spectral variation of the dune surface.

The cos α dependency in raw mode (Figures 4 and 5) is due to the relative significance of the additive path radiance, offset, and skylight terms compared to the magnitude of the information term in numerator and denominator (see Equations 1 and 2). We create ratio variables with the shorter wavelengths in the denominator. Therefore, the additive terms of the denominator are larger than those of the numerator because the path radiance and skylight terms are larger for shorter wavelength bands in the visible and near-infrared region—atmospheric scattering increases toward shorter wavelengths. With a decrease of cos α from 1.0 to 0.0, the large additive term in the denominator causes progressively smaller ratio values because the information term of Equation 1 decreases. In other words, as cos α decreases, the constant additive terms exert a relatively greater effect on the outcome of the ratio values and the ratio values drop. If ratio variables are created with the shorter wavelength in the numerator (e.g., Landsat 4/5), the raw ratio values will increase as cos α decreases. Note also that the system offset term (OF_c of Equation 1) of the Landsat-1 and -2 data studied here is small compared to the combined path radiance and skylight terms. This may not be the case for other sensor systems because the size of the offset term is governed by engineering considerations. If the offset term of one band dominates the other additive terms, the raw ratio values will respectively either increase or drop with decrease of cos α according to whether the dominating offset term occurs in the numerator or denominator of the ratio.

Most topographic surfaces fall within the range of cos α from 0.35 to 1.00 under the high sun elevation angle (56 degrees) during imaging on 1 June 1977 (for example, see Figure 3). A steep slope of 35 degrees facing directly away from the sun would have a cos α value of 0.35. Most sites would have larger cos α values. The model results (Figures 4 and 5) show that the 5/4 and 6/4 ratios increase by about 0.35 and 0.40 ratio units, respectively, between cos α from 0.35 to 1.00. This variation is significant because the mean ratio values of limonitic rock sites and other rock sites in the Landsat data from the Yerington District are commonly separated by only 0.10 to 0.30 ratio units. This difference between rock types is the same order of magnitude as the variability due to the modeled surface topographic effect.

After a PRC, the ratio values are much less dependent upon the surface orientation, especially across the range of cos α from about 0.35 up to 1.00 (Figures 4 and 5). Across the entire range of cos α, the new ratios for each surface take on a larger range of values than do the PRC ratios by a factor of 2×. Across the range of cos α occupied by common topographic surfaces under these high sun angle conditions (cos α greater than or equal to 0.35), the range of raw 5/4 ratios is 6× greater than the range of the PRC ratios. The 5/4 values for the limonitic quartz monzonite, for example, range from 1.32 to 1.62 in raw mode, but only from 1.92 to 1.97 in corrected mode across the range of cos α = 0.35 to 1.00.

Note that, in support of the modeled results, the PRC subdues the variation of the ratio values in the traverse of the sand dune (Figure 6). Some residual variation remains and may be due to a combination of the skylight term, an imperfect PRC, and noise in the data.

The model results show that the topographic orientation of the surface affects the discrimination among the rock types when ratios are used. For example, the limonitic quartz monzonite surface has larger raw 5/4 values (Figure 4) at any given cos α than do the other three sites, and may be separable from them on that basis. At cos α = 0.80, the limonitic site is larger in 5/4 by about 0.17 ratio units. However, a poorly illuminated limonitic pixel having cos α less than or equal to 0.50 will have raw 5/4 values which are as low as, or lower than, the raw 5/4 values from pixels of the other

three surfaces which are at cos α greater than or equal to 0.80. Thus, on the basis of the 5/4 ratio, the poorly illuminated limonitic site will be confused with surfaces of the other rock types that happen to occur on well illuminated topographic slopes during imaging. *This effect is significant in attempts to remotely identify limonitic outcrops, and explains the common observation when using raw ratio data of (1) false high-ratio anomalies on well illuminated, bright but nonlimonitic slopes, and (2) the absence of limonitic anomalies on poorly illuminated slopes where limonitic rocks are known to occur.* The authors observed the former case in study of the Granite Mountains area of the Mojave Desert and in the Alaska Range, Alaska. Krohn et al. (1978) described an example of the latter case in the Battle Mountain District, Nevada.

Furthermore, we can infer that in areas where the rock types are not spectrally very distinct in the available wavelength bands, but have local characteristic topographic expression, the cos α effect present in raw ratios may artificially aid the rock type discrimination. Using PRC ratios, the same area may appear spectrally more bland because the topographic effect has been removed. Thus, the discrimination obtained with raw ratio values may be adversely subdued by the correction.

Notice that the ratios of digital numbers in Figures 4 and 5 are larger than the ratios of the respective reflectance values. This is because the constant multiplicative factor due to the irradiance, transmittance, and system gains happens to be larger than 1.00 for each ratio. Also, the ratio values are larger after a PRC because a larger path radiance estimate is subtracted from the band in the denominator than from the numerator. The fact that the radiance ratios are different from the reflectance ratios, particularly after a PRC, does not mean that the radiance ratios are therefore less useful or less descriptive of the surface than are the reflectance ratios. The radiance ratios are proportional to the reflectance ratios by a multiplicative constant, provided that the additive terms are negligible or corrected.

The remaining variation in the modeled ratio values after PRC (Figures 4 and 5) is caused by the skylight term. Pixels in hilly terrain which are poorly illuminated by direct sunlight have the skylight as a relatively larger fraction of their irradiance than do well illuminated pixels. The spectral character of such poorly illuminated surfaces is represented by lower ratio values. A correction for the additive skylight term would remove the remaining variation in 5/4 and 6/4 ratio values in Figures 4 and 5. For these model parameters and 56-degree sun elevation angle, the skylight correction would primarily affect the rare and exceedingly steep slopes which face away from the sun. A perfect skylight correction to the 1 June 1977 data would therefore have a minimal effect because very few sites have cos α low enough to be affected more than marginally (Figures 3, 4, and 5).

On images recorded at lower sun elevation angles, the skylight effect will be larger than that shown in Figures 4 and 5 because the skylight will be a larger proportion of the total irradiance. The skylight effect will also be more significant because the cos α distribution will range down to low values and may go negative (Figure 3). For example, the cos α value for a 35-degree slope facing directly away from the sun at 40-degree elevation is 0.09, whereas at 56-degree sun elevation, the cos α value is much larger, 0.35. A skylight correction was attempted in Kowalik, (1981).

DISCRIMINANT ANALYSES

We use linear discriminant analysis in a geological context to evaluate the effect of a PRC on Landsat data. The evaluation is based on (1) the overall classification rates before and after correction, and (2) the study of the topographic characteristics of the sites that are incorrectly classified.

Linear discriminant analysis defines a function based on a linear combination of variables to maximize the separability of samples representing two or more known groups. Classification functions associated with the discriminant function can be used to classify unknown samples into one of the known groups. Davis (1973), Johnston (1978), and Conel *et al.* (1978) provide introductory explanations of discriminant analysis.

We used the BMDP7M stepwise linear discriminant program (Dixon and Brown, 1977). The BMDP7M program operates in a stepwise fashion and chooses variables to enter or remove from the function at each step based upon the F statistic (among group variance/within group variance). The variable with the largest F at any step is entered into the linear function, provided the F is above a minimum cutoff level. The cutoff was set to 4.0 in these analyses and all six ratio variables of Landsat data (5/4, 6/4, 6/5, 7/4, 7/5, 7/6) were available to enter the discriminant function.

The program can determine the class to which each sample belongs by using a classification function for each sample which does not include the particular sample about which a decision is being made. These so-called jackknifed classification accuracies are less biased than are accuracies that are obtained by including the sample (about which a decision is being made) in the pool of samples used to derive and assess the classification accuracy.

We obtained a sample of 183 noncontiguous, one-pixel sized sites representing three broad rock types, (1) limonitic quartz monzonite (Lqm), (2) nonlimonitic plutonic rocks (Nlp), and (3) volcanic

rocks, from each of six Landsat data sets (Table 1) of the Yerington District, Nevada (Figure 1). We located the sites on large-scale color aerial photography and transferred their locations to USGS orthophotoquads. We then located the sites in each of the six Landsat data matrices by overlaying 1:24,000 scale dotprints onto the orthophotoquads and extracted the data values by bilinear interpolation. Each data set was subdivided by odd and even ID# into two data sets ($6 \times 2 = 12$ total data sets) to help assess the reproducibility of the classification results.

The topographic slope of each site was measured in the field. The cos α distribution of the 183 sites for each of the six Landsat overpasses is shown in Figure 3.

The study area that we sampled is confined to a relatively small subscene (6-km EW by 15-km NS) within the Landsat image (Figure 1) in the semiarid western Nevada area. Restriction to a small area minimizes the geographic variation of the atmospheric parameters. Also, we are not concerned with the time dimension. The six different Landsat data sets used here are analyzed independently of each other. No attempt has been made to transfer spectral signatures from one image to another image recorded at a different time.

RESULTS OF DISCRIMINANT ANALYSES

Table 3 summarizes the jackknifed classification using raw and path radiance corrected data: (1) Lqm versus Nlp and (2) Lqm versus volcanic rocks. We obtained estimates of the path radiance for each Landsat data set by an optimization algorithm that uses Mahalanobis distances between the sampled groups as described by Kowalik (1981). When other more conventional methods for estimating PRC values are used (Chavez, 1975; Switzer *et al.*, 1981), the results are similar to those presented in Table 3 (Kowalik, 1981).

After PRC, the classification accuracy of the Lqm versus Nlp rock sites increased by an average of 10 percent, from 87 percent to 97 percent. The accuracy improved because after correction (1) the *poorly illuminated* Lqm sites are more often correctly classified as Lqm and (2) the *well illuminated* Nlp sites are more often correctly classified as Nlp (see Table 4). We inferred this result earlier from the model (Figures 4 and 5). The cos α dependence is subdued after correction and the Lqm curve is distinctly more separate from the Nlp curve in those figures.

Table 4 summarizes the mean cos α values of the sites that were misclassified when raw data were used and when PRC data were used. Cos Z in Table 4 is the cos α value for a horizontal site and can be used as a marker point to assess the degree of illumination associated with other cos α values: i.e., other nonhorizontal sites are either better illuminated (cos $\alpha >$ cos Z) or more poorly illuminated (cos $\alpha <$ cos Z).

Table 4 shows that the misclassified Lqm sites are poorly illuminated and the misclassified Nlp sites tend to be well illuminated, both in raw data and after PRC. For each data set, the number of misclassifications drops markedly after the PRC. After PRC, some sites are still misclassified, perhaps because an imperfect correction was applied, and because of noise in the data, especially at low levels of illumination (low cos α).

The discrimination of Lqm from the volcanic rock group (Table 3) with Landsat ratio variables is not very accurate (70 percent correct). This is due to the overall spectral similarity of the Lqm and volcanic rock groups in the Landsat wavelength bands (Kowalik, 1981). The classification accuracy

TABLE 3. JACKKNIFED CLASSIFICATION ACCURACIES

Landsat Data Sets	Lqm vs Nlp Subgroup A n = 42 Subgroup B n = 43 Raw Ratios	Lqm vs Nlp Subgroup A n = 42 Subgroup B n = 43 PRC Ratios	Lqm vs Volcanic Rocks Subgroup A n = 79 Subgroup B n = 77 Raw Ratios	Lqm vs Volcanic Rocks Subgroup A n = 79 Subgroup B n = 77 PRC Ratios
9/16/72 A	83.3	100.0	68.4	72.2
9/16/72 B	88.4	95.3	70.1	72.7
5/26/73 A	85.7	97.6	68.4	73.4
5/26/73 B	93.0	100.0	66.2	72.7
6/1/77 A	95.2	100.0	72.2	74.7
6/1/77 B	97.7	100.0	76.6	76.6
8/30/77 A	92.9	95.2	77.2	77.2
8/30/77 B	95.3	100.0	80.5	79.2
10/5/77 A	92.9	97.6	77.2	73.4
10/5/77 B	83.7	95.3	59.7	59.7
11/10/77 A	69.0	92.9	51.9	55.7
11/10/77 B	72.1	95.3	59.7	63.6
$\bar{\chi}$	87.4	97.4	69.0	70.9
s	9.2	2.6	8.6	7.3

TABLE 4. MEAN COS α VALUES OF MISCLASSIFIED Lqm AND Nlp SITES

Landsat Data Set	cos Z	Sites that were Misclassified as Nlp: Raw data cos α	Raw data n	PRC data cos α	PRC data n	Sites that were Misclassified as Lqm: Raw data cos α	Raw data n	PRC data cos α	PRC data n
9/16/72	0.72	0.49	6	0.42	1	—	0	—	0
5/26/73	0.87	0.78	5	0.90	1	0.88	4	—	0
6/1/77	0.83	0.81	2	—	0	—	0	—	0
8/30/77	0.71	0.53	5	0.68	2	—	0	—	0
10/5/77	0.58	0.33	5	0.30	2	0.48	2	0.66	1
11/10/77	0.43	0.17	16	0.18	2	0.57	7	0.46	3

is also essentially unchanged by the PRC, a result that we could have inferred from the model. At cos $\alpha = 0.80$, the difference in raw 5/4 ratios between the Lqm and hematitic tuff is 0.16 ratio units and, after a PRC, the difference is 0.19 units (Figure 4). We could expect, however, that, if the tuff sites and Lqm sites occurred at group specific ranges of cos α, the raw ratios could provide a better discrimination than the PRC ratios.

CONCLUSIONS

The model predicts that a residual surface orientation effect is present in raw ratios of Landsat data due primarily to the additive path radiance term. The skylight term has a smaller effect which we consider to be negligible for the conditions modeled. A path radiance correction will remove a large part of that residual orientation effect and in hilly terrain will reduce confusion between rock types that are spectrally different. In the example studied, results of linear discriminant analyses concur with predictions from the model and specifically show that a path radiance correction subdues tendencies for (1) poorly illuminated limonitic quartz monzonite sites to be misclassified with the nonlimonitic plutonic rock group, and (2) well illuminated nonlimonitic sites to be classified incorrectly with the limonitic group.

We infer from results of the model that raw ratio variables can provide a better separation of rock types which are spectrally similar and which occur at group-specific, characteristic topographic orientations. The separation achieved in such a case with raw ratios would be due to the characteristic topographic orientation of each group, and not to the spectral character of the rock types. Application of a PRC in that case would subdue the topographic effect that causes the separation, and the rock types would appear to be less separable. However, in spectral exploration with Landsat data, it is commonly desirable that the ratio values of Landsat data should correspond to the reflectance ratios of the surface materials, and not to a combination of surface reflectance and surface topographic orientation. To achieve this end, a path radiance correction is necessary prior to creating ratio variables.

ACKNOWLEDGMENT

The senior author wishes to thank the USGS, EROS Program for part-time support during this research.

REFERENCES

Ballew, G. I., 1975. *A Method for Converting Landsat-1 MSS Data to Reflectance by Means of Ground Calibration Sites:* Stanford Remote Sensing Lab Report 75-5, 50 p.

Chavez, P. S., Jr., 1975. Atmospheric, Solar, and MTF Corrections for ERTS Digital Imagery: *Proc. of Am. Soc. Photogrammetry,* Falls Church, Va., Oct., p. 69a.

Chavez, P. S., Jr., and W. B. Mitchell, 1977. Computer Enhancement Techniques of Landsat MSS Digital Images for Land Use/Land Cover Assessments: *Proceedings of 6th Annual Remote Sensing of Earth Resources Conference,* March 29-31, pp. 259-276.

Conel, J. E., M. J. Abrams, and A. F. H. Goetz, 1978. *A Study of Alteration Associated with Uranium Occurrences in Sandstones and its Detection by Remote Sensing Methods:* JPL Publication 78-66, v. 1, 2.

Davis, J. C., 1973. *Statistics and Data Analysis in Geology:* John Wiley and Sons, Inc., pp. 93-99.

Dixon, W. J., and M. B. Brown, 1977. BMDP-77, *Biomedical Computer Programs, P-Series:* University of California Press, Berkeley, 880 p.

Hunt, G. R., J. W. Salisbury, and C. J. Lenhoff, 1971. Visible and Near-Infrared Spectra of Minerals and Rocks: III Oxides and Hydroxides: *Modern Geology,* v. 2, pp. 195-205.

Hunt, G. R., and R. P. Ashley, 1979. Spectra of Altered Rocks in the Visible and Near-Infrared: *Economic Geology,* v. 74, pp. 1613-1629.

Johnston, R. J., 1978. *Multivariate Statistical Analysis in Geography:* Longman, London and New York, 280 p.

Knopf, A., 1918. *Geology and Ore Deposits of the Yerington District, Nevada:* U.S. Geological Survey Professional Paper 114, 192 p.

Kowalik, W. S., 1981. *Atmospheric Corrections to Landsat Data for Limonite Discrimination:* Ph.D. Dissertation, Stanford University, 365 p.

Kowalik, W. S., S. E. Marsh, and R. J. P. Lyon, 1982. *A*

Relationship Between Landsat Digital Numbers, Surface Reflectance, and the Cosine of the Solar Zenith Angle: Remote Sensing of Environment, v. 12, pp. 39-55.

Kriegler, F. J., W. A. Malila, R. F. Nalepka, and W. Richardson, 1969. Preprocessing Transformations and Their Effects on Multispectral Recognition: *Proceedings of 6th International Symposium on Remote Sensing of Environment,* v. 1, pp. 97-131.

Krohn, M. D., M. J. Abrams, and L. C. Rowan, 1978. *Discrimination of Hydrothermally Altered Rocks Along the Battle Mtn.-Eureka Nevada Mineral Belt Using Landsat Images:* U.S. Geological Survey Open-File Report 78-585, 66 p.

Lyon, R. J. P., F. R. Honey, and G. I. Ballew, 1975. A Comparison of Observed and Model-Predicted Atmospheric Perturbations on Target Radiances Measured by ERTS: Part I—Observed Data and Analysis: *Proceedings of IEEE Conference on Decision and Control,* Houston, Texas, December 2-10, pp. 244-249.

Malila, W. A., R. C. Cicone, and J. M. Gleason, 1976. *Wheat Signature-Modeling and Analysis for Improved Training Statistics:* Final Report to NASA, ERIM Report 109600-66-F, 170 p.

Marsh, S. E., 1978. *Quantitative Relationships of Surface Geology and Spectral Habit to Satellite Radiometric Data:* Ph.D. Dissertation, Stanford University, 225 p.

Moore, J. G., 1969. *Geology and Mineral Deposits of Lyon, Douglas, and Ormsby Counties, Nevada:* Nevada Bureau of Mines and Geology, Bulletin 75, 45 p.

Otterman, J., S. Ungar, Y. Kaufman, and M. Podolak, 1980. Atmospheric Effects on Radiometric Imaging from Satellites Under Low Optical Thickness Conditions: *Remote Sensing of Environment,* v. 9, pp. 115-129.

Proffett, J. M., Jr., 1977. Cenozoic Geology of the Yerington District, Nevada, and Implications for the Nature and Origin of Basin and Range Faulting: *Geological Society American Bulletin,* v. 88, pp. 247-266.

Reeves, R. G., *et al.,* eds., 1975. *Manual of Remote Sensing:* American Society of Photogrammetry, p. 91.

Robinove, C. J., and P. S. Chavez, Jr., 1978. Landsat Albedo Monitoring for an Arid Region: Paper presented at the AAAS International Symposium on Arid Region Plant Resources, Lubbock, Texas, 24 p.

Rogers, R. H., and K. Peacock, 1973. A Technique for Correcting ERTS Data for Solar and Atmospheric Effects: *Symposium of Sig. Results Obtained from the ERTS-1,* Mar. 5-9, New Carrollton, Md., pp. 1115-1122.

Rowan, L. C., P. H. Wetlaufer, A. F. H. Goetz, F. C. Billingsley, and J. H. Stewart, 1975. *Discrimination of Rock Types and Detection of Hydrothermally Altered Areas in South Central Nevada by the Use of Computer Enhanced ERTS Images:* U.S. Geological Survey Professional Paper 883, 35 p.

Rowan, L. C., A. F. H. Goetz, and R. P. Ashley, 1977. Discrimination of Hydrothermally Altered and Unaltered Rocks in Visible and Near Infrared Multispectral Images: *Geophysics,* v. 42, 3, pp. 522-535.

Selby, J. E. A., F. X. Kneizys, J. H. Chetuynd, Jr., and R. A. McClatchey, 1978. *Atmospheric Transmittance/Radiance: Computer Code Lowtran 4:* U.S. Air Force Cambridge Res. Lab., Env. Res. Paper No. 626, 100 p.

Slater, P. N., 1980. *Remote Sensing, Optics and Optical Systems:* Addison-Wesley Publishing Co., Reading, Mass., 579 p.

Smedes, H. S., M. M. Spencer, and F. J. Thomson, 1971. Preprocessing of Multispectral Data and Simulation of ERTS Data Channels to Make Computer Terrain Maps of a Yellowstone National Park Test Site: *Proceedings of 7th International Symposium on Remote Sensing of Environment,* pp. 2073-2094.

Switzer, P., W. S., Kowalik, and R. J. P. Lyon, 1981. Estimation of Atmospheric Path Radiance by the Covariance Matrix Method, *Photogrammetric Eng. and Remote Sensing:* v. 57, 10, pp. 1469-1476.

Turner, R. E., 1975. Signature Variations Due to Atmospheric Effects: *Proceedings of 10th International Symposium on Remote Sensing of Environment,* pp. 671-682.

USGS, 1979. *Landsat Data Users Handbook,* p. AE-16.

Vincent, R. K., 1973. Ratio Maps of Iron Ore Deposits Atlantic City District, Wyoming: *Symposium on Sig. Results Obtained from the ERTS-1,* Mar. 5-9, New Carrollton, Md., pp. 379-386.

———, 1977. Uranium Exploration with Computer Processed Landsat Data: *Geophysics,* v. 42, 3, pp. 536-541.

(Received 21 July 1981; revised and accepted 4 January 1983)